Acta Crystallographica Section B
Structural Science
ISSN 0108-7681

$[Rh(C_7H_8)(PPh_3)Cl]$: an experimental charge-density study

Hazel A. Sparkes,[a] Simon K. Brayshaw,[b] Andrew S. Weller[c] and Judith A. K. Howard[a]*

[a]Department of Chemistry, Durham University, University Science Laboratories, South Road, Durham DH1 3LE, England, [b]Department of Chemistry, University of Bath, Claverton Down, Bath BA2 7AY, England, and [c]Department of Inorganic Chemistry, University of Oxford, South Parks Road, Oxford OX1 3QR, England

Correspondence e-mail: j.a.k.howard@durham.ac.uk

Received 23 April 2008
Accepted 15 August 2008

In order to gain a deeper understanding into the bonding situation in rhodium complexes containing rhodium–carbon interactions, the experimental charge-density analysis for $[Rh(C_7H_8)(PPh_3)Cl]$ (1) is reported. Accurate, high-resolution ($\sin\theta/\lambda = 1.08$ Å^{-1}), single-crystal data were obtained at 100 K. The results from the investigation were interesting in relation to the interactions between the rhodium metal centre and the norbornadiene fragment and illustrate the importance of such analyses in studying bonding in organometallic complexes.

1. Introduction

Accurate, high-resolution X-ray charge-density experiments provide information on the electron distribution within the system under study, allowing both the nature of the bonding and the atomic interactions to be determined. To this end, Bader's quantum theory of atoms in molecules (AIM; Bader, 1990) is a powerful tool, which characterizes the chemical interactions between atoms on the basis of the topological properties of the electron density [$\rho(r)$] and the associated Laplacian [$\nabla^2\rho(r)$] at bond-critical points (b.c.p.s; Bader & Essén, 1984). In organometallic compounds, shared-shell interactions, such as covalent bonds, are characterized by positive values of $\rho(r)$ and negative values of $\nabla^2\rho(r)$ at the b.c.p.s, while closed-shell interactions, such as ionic bonding, van der Waals and hydrogen bonding, tend to have small positive values for both $\rho(r)$ and $\nabla^2\rho(r)$ at the b.c.p.s.

Transition metal complexes have important applications in many areas of catalysis and they are also well known to promote the cleavage of C—C bonds. The latter application is particularly useful in organic synthesis as it allows strong C—C bonds to be broken and subsequently functionalized (Jun, 2004). One way in which to achieve metal promoted C—C activation is through the use of intrinsically strained species such as cyclopropanes (Rybtchinski & Milstein, 1999). In such a system, the driving force to overcome the thermodynamic and kinetic barriers to the cleavage of C—C bonds is thought to be the reduction of strain. Our current interest in rhodium complexes arises from their potential C—C bond-activation properties, such processes passing through putative intermediates that have Rh···C—C sigma interactions. $[Rh(PR_3)(binor\text{-}S)][BAr^F_4]$ is a rare example of such an intermediate which we have recently structurally characterized by X-ray diffraction at 150 K (Brayshaw *et al.*, 2007) [$Ar^F = C_6H_3(CF_3)_2$]. Complexes of the type $Rh(C_7H_8)(PR_3)Cl$ (R = alkyl or aryl) are useful precursors in the synthesis of these intermediate complexes. In order to gain a deeper understanding of the nature of the bonding in rhodium complexes containing Rh···C—C interactions we have

Table 1
Experimental details.

Crystal data	
Chemical formula	$C_{25}H_{23}ClPRh$
M_r	492.76
Cell setting, space group	Triclinic, $P\bar{1}$
Temperature (K)	100 (2)
a, b, c (Å)	10.2430 (1), 10.4042 (1), 11.4078 (1)
α, β, γ (°)	99.213 (1), 103.131 (1), 115.080 (1)
V (Å^3)	1026.01 (2)
Z	2
D_x (Mg m^{-3})	1.595
μ (mm^{-1})	1.05
Reflections collected	370 693
Independent reflections	21 647
R_{int}	0.0376
Completeness to θ = 50.14°	100%
Spherical-atom refinement	
No. of data in refinement	21 647
No. of refined parameters	345
GOF (F^2)	1.069
Final R_1 [$F^2 > 2\sigma(F)$] (all data)	0.0164 (0.0186)
wR_2 [$F^2 > 2\sigma(F)$] (all data)	0.0437 (0.0443)
Largest difference peak/hole (e Å^{-3})	0.666/−1.064
Multipole refinement	
No. of data in refinement (N_{ref})	19 920
No. of refined parameters (N_v)	514
N_{ref}/N_v	38.8
GOF (F)	1.353
Final R_1 [$I > 2\sigma(I)$] (all data)	0.0117 (0.0154)
wR_2 [$I > 2\sigma(I)$]	0.0116
Largest difference peak/hole (e Å^{-3})	0.329/−0.318

Computer programs used: *COLLECT* (Nonius BV, 1999), *HKL DENZO/SCALEPACK* (Otwinowski & Minor, 1997), *SHELXS*97 (Sheldrick, 2008), *XD* Volkov *et al.* (2006).

conducted an experimental charge-density study on the title complex (1), $Rh(C_7H_8)(PPh_3)Cl$, at 100 K (C_7H_8 = norbornadiene). Herein we present the results of this investigation with particular focus on the bonding around the rhodium metal centre. Although this organometallic complex displays Rh–alkene bonding interactions with the organic fragment, as opposed to metal–alkane sigma interactions, these studies serve as an excellent baseline marker for future investigations into systems with the more exotic bonding motifs.

2. Experimental

2.1. Synthesis

[$Rh(C_7H_8)(PPh_3)Cl$] (1) was synthesized following the published methods (Bennett & Wilkinson, 1961). Single crystals suitable for charge-density analysis were obtained by diffusion of pentane into a concentrated solution of the complex in dichloromethane.

2.2. Data collection and spherical-atom refinement

Two high resolution, single-crystal X-ray diffraction datasets were recorded from two different crystals of (1) on a Nonius Kappa CCD diffractometer using graphite-monochromated Mo $K\alpha$ radiation (λ = 0.71073 Å) at 100(2) K. The data were collected using the strategy calculated by the *COLLECT* software (Nonius, 1999) and integrated using *HKL SCALEPACK* (Otwinowski & Minor, 1997). Details of the two data collections are summarized in Table S1 of the supplementary data.[1] Both data collections were from good quality crystals, however, in the first data collection an oversized beam stop was employed and hence the six lowest angle reflections were not measured; as a result this data was only used above sin θ/λ = 0.2 Å^{-1}. The variation of the scale factor *versus* resolution for the two datasets were within acceptable limits of around ±3%, see Fig. S1. Data from the two crystals were merged and corrected for absorption using *SORTAV* (Blessing, 1997) within the *WinGX* suite (Farrugia, 1999). A total of 370 693 measured reflections were merged to give 21 647 unique reflections which had an R_{int} of 0.038 and were 100% complete to sin θ/λ = 1.08 Å^{-1}. A plot of scale factor *versus* resolution for the combined data was satisfactory with a maximum variation of ±3% around unity, see Fig. S2.

The structure was solved using direct methods (*SHELXS*97; Sheldrick, 2008) and refined by full-matrix least squares on F^2 (*SHELXL*97; Sheldrick, 2008). H atoms were located in the difference Fourier map and refined freely. The structure obtained was consistent with that previously reported in the literature (Takenaka & Osakada, 2000).

2.3. Multipole refinement

The *XD*2006 program suite (Volkov *et. al.* 2006), which implements the multipole formalism of Hansen & Coppens (1978), was employed for an aspherical-atom refinement, using the spherical-atom model obtained above as the starting point. All of the available and appropriate aspherical-atom databanks were tested in order to obtain the best refinement, however, the final results were essentially indistinguishable from each other. STO-Dirac-Fock atomic relativistic wavefunctions (Su & Coppens, 1998; Macchi & Coppens, 2001) were used in the final refinement. The importance of including relativistic effects for second-row transition metals has been highlighted recently and affects the accuracy of the topological parameters at the critical point (Eickerling *et al.*, 2007). The electronic configuration $5s^1 4d^8$ was used for rhodium with the $5s^1$ scattering contribution fixed as part of the core contribution. Initially only the scale factor was refined, followed by the atomic positions and displacement parameters. Subsequently, a high-order refinement (sin $\theta/\lambda > 0.7$ Å^{-1}) was carried out to determine the optimal atomic positions and displacement parameters for the non-H atoms after which the scale factor was fixed. This was followed by a low-order refinement (sin $\theta/\lambda < 0.7$ Å^{-1}) of the positional and isotropic displacement parameters of the H atoms; the isotropic displacement parameters were then fixed after the refinement reached convergence. In all further refinement cycles, the C—H bond lengths were reset to their average neutron diffraction distances of 1.08 (aromatic) and 1.10 Å (C_7H_8 cage). The multipole expansion was truncated at the hexadecapole level for rhodium, phosphorus and chlorine, the octupole level for

[1] Supplementary data for this paper are available from the IUCr electronic archives (Reference: BS5064). Services for accessing these data are described at the back of the journal.

all C atoms and the bond-directed dipole level for the H atoms. The H atoms were assigned to four groups (aromatic, methylene, vinyl and those attached to C3/C6) and the CHEMCON constraint in *XD* was applied to the groups to keep their valence deformation densities the same. The CHEMCON constraint was also applied to the aromatic C atoms which were divided into three groups depending on whether they were in the *ortho*, *meta* or *para* positions of the ring. The charge on the complex was maintained using the command KEEP charge group 1. Five κ parameters were refined for all atom types along with four κ' parameters for the non-H atoms, the κ' parameters were constrained to be the same for all multipoles. An isotropic extinction parameter was refined, which produced a small but significant improvement in the refinement, so it was included in the final refinement. The residual-density map, at the end of the refinement using all data, was almost featureless with maximum residuals of 0.329 and -0.318 e Å^{-3}, which were located around the rhodium atom as expected, see Figs. S3 and S4 in the supplementary information. The Hirshfeld rigid-bond test (Hirshfeld, 1976) carried out after the multipole refinement was satisfactory (Table S2). All the Rh1—C bonds had significantly higher maximum mean-square atomic displacements along the bond directions (22–23 $\times 10^{-4}$ Å^2) than found for the rest of the bonds in the complex for which the highest value was 11 $\times 10^{-4}$ Å^2 for Rh1—Cl1, the reasons for this are discussed later. Further details of the experimental data collection and refinement are provided in Table 1.

3. Results and discussion

Fig. 1 shows an *ORTEP* plot of (1) with the H atoms omitted for clarity. The compound contains triphenylphosphine, chloride and norbornadiene ligands all bound to a square-planar rhodium metal centre which is formally in the +1 oxidation state. The topological properties at the critical points identified for the complex are listed in Table 2. Examining the topological properties relating to the triphenylphosphine ligand showed nothing remarkable, the bonding around each of the phenyl rings was as expected covalent [with positive values of $\rho(r)$ ranging from 2.07 (1) to 2.14 (1) e Å^{-3} and negative values for the Laplacian ranging from -18.02 (2) to -20.18 (2) e Å^{-5} at the b.c.p.s]. The bond lengths and ellipticities (ε) are consistent with aromatic delocalized bonding as anticipated, and three ring critical points (r.c.p.s) were identified. Each of the phosphorus–carbon bonds is also a shared-shell covalent interaction. The smaller values of $\rho(r)$ and $\nabla^2\rho(r)$ compared with the aromatic carbon–carbon bonds suggest that less electron density is located in these bonds, which combined with the smaller ellipticities indicate that the P—C bonds have less π character, as expected.

A comparison of the interatomic distances and angles around the norbornadiene ligand in (1) and the free ligand (Benet-Buchholz *et al.*, 1998) found in the Cambridge Structural Database (Allen, 2002) is shown in Table 3. The majority of the bond lengths and angles found in (1) are fairly similar to those in the free norbornadiene ligand. However, it is worth noting that upon coordination to the rhodium metal centre, two significant changes are seen; firstly the length of the two formal double bonds (C1═C2 and C4═C5) increase by approximately 0.05 and 0.08 Å, respectively [as expected from the classical Chatt–Dewar–Duncanson (Dewar, 1951; Chatt & Duncanson, 1953) model for bonding between an alkene and a late-transition metal (Crabtree, 2005) based on a suitable combination of symmetry-related orbitals on the metal and alkene]. Secondly the angles C2—C3—C4 and C5—C6—C1 reduce by *ca* 6° in order to facilitate coordination of the norbornadiene to the metal centre. Despite the increase in the C1═C2 and C4═C5 bond lengths, they have a higher electron

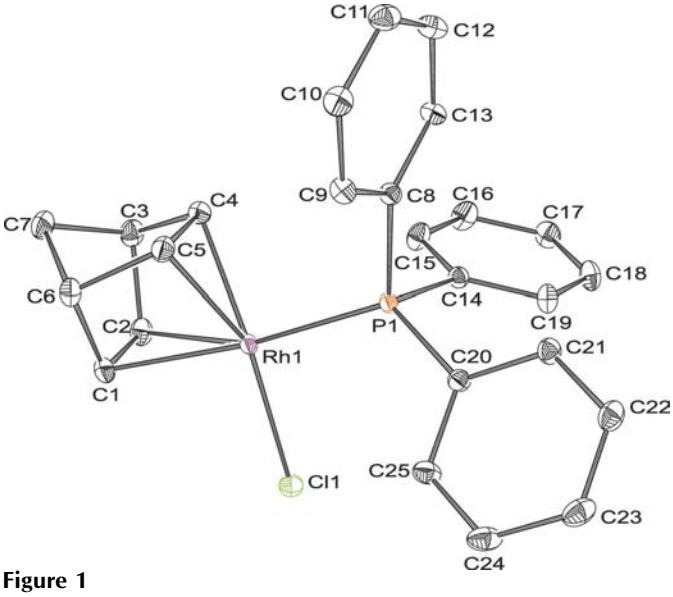

Figure 1
ORTEP plot for [Rh(C_7H_8)(PPh_3)Cl] with ellipsoids depicted at the 50% level. H atoms are omitted for clarity.

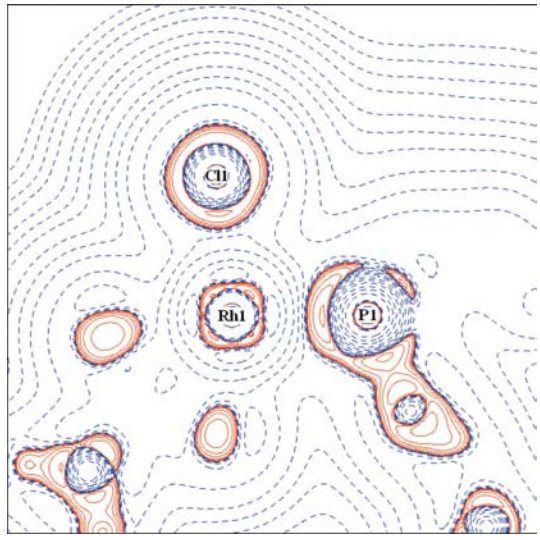

Figure 2
Laplacian of the electron density for (1) drawn in the plane of Rh1—P1—Cl1, positive contours are solid red lines, while negative contours are dashed blue lines.

Table 2
Topological properties at the b.c.p.s and selected r.c.p.s in $[Rh(C_7H_8)(PPh_3)Cl]$ (1).

Bond	d_{ij} (Å)	R_{ij} (Å)†	$\rho(r_{b.c.p.})$ (e Å^{-3})	$\nabla^2\rho(r_{b.c.p.})$ (e Å^{-5})	λ_1	λ_2	λ_3	ϵ
Rh1—C1	2.2193 (3)	2.3061	0.574 (4)	5.497 (4)	−2.02	−0.38	7.89	4.39
Rh1—C2	2.2192 (3)	–	–	–	–	–	–	–
Rh1—C4	2.1087 (3)	2.1347	0.742 (6)	6.731 (7)	−3.06	−0.77	10.57	2.96
Rh1—C5	2.1058 (3)	2.1531	0.737 (6)	6.890 (6)	−3.07	−0.49	10.45	5.28
Rh1—P1	2.3034 (1)	2.3039	0.677 (6)	3.410 (6)	−2.38	−2.03	7.82	0.17
Rh1—Cl1	2.3625 (1)	2.3627	0.570 (3)	6.429 (3)	−2.07	−1.85	10.35	0.11
P1—C8	1.8322 (2)	1.8330	1.16 (1)	−7.88 (3)	−6.37	−5.61	4.11	0.14
P1—C14	1.8287 (2)	1.8292	1.14 (1)	−7.70 (3)	−6.09	−5.43	3.83	0.12
P1—C20	1.8242 (2)	1.8245	1.14 (1)	−7.81 (3)	−5.87	−5.59	3.66	0.05
C1—C2	1.3845 (4)	1.3861	2.20 (2)	−18.74 (4)	−16.55	−13.09	10.90	0.26
C1—C6	1.5386 (4)	1.5387	1.61 (1)	−8.99 (3)	−10.81	−9.44	11.26	0.15
C2—C3	1.5390 (5)	1.5397	1.64 (1)	−9.46 (3)	−10.97	−9.91	11.43	0.11
C3—C4	1.5449 (5)	1.5459	1.55 (1)	−8.31 (3)	−10.10	−8.99	10.78	0.12
C3—C7	1.5497 (4)	1.5507	1.57 (1)	−8.22 (3)	−9.92	−9.49	11.18	0.05
C4—C5	1.4164 (4)	1.4173	1.98 (2)	−13.86 (4)	−14.38	−10.61	11.13	0.36
C5—C6	1.5416 (4)	1.5423	1.60 (1)	−8.72 (3)	−10.52	−9.38	11.19	0.12
C6—C7	1.5478 (5)	1.5480	1.52 (1)	−7.96 (3)	−9.49	−9.24	10.77	0.03
C8—C9	1.4059 (3)	1.4060	2.08 (1)	−18.05 (2)	−15.66	−13.01	10.62	0.20
C8—C13	1.3991 (3)	1.3992	2.08 (1)	−18.03 (2)	−15.85	−12.74	10.56	0.24
C9—C10	1.3952 (4)	1.3953	2.12 (1)	−19.66 (2)	−16.45	−13.51	10.29	0.22
C10—C11	1.3972 (4)	1.3973	2.13 (1)	−19.79 (2)	−16.57	−13.59	10.38	0.22
C11—C12	1.3948 (4)	1.3948	2.13 (1)	−19.73 (2)	−16.43	−13.57	10.27	0.21
C12—C13	1.3972 (4)	1.3973	2.13 (1)	−19.52 (2)	−16.50	−13.48	10.46	0.22
C14—C15	1.4021 (3)	1.4024	2.09 (1)	−18.35 (2)	−15.80	−13.08	10.53	0.21
C14—C19	1.3995 (3)	1.3995	2.08 (1)	−18.02 (2)	−15.85	−12.74	10.57	0.24
C15—C16	1.3947 (4)	1.3947	2.14 (1)	−19.67 (2)	−16.57	−13.52	10.42	0.23
C16—C17	1.3918 (4)	1.3918	2.14 (1)	−20.18 (2)	−16.59	−13.74	10.15	0.21
C17—C18	1.3899 (4)	1.3899	2.14 (1)	−20.15 (2)	−16.60	−13.70	10.15	0.21
C18—C19	1.3944 (3)	1.3944	2.14 (1)	−19.76 (2)	−16.61	−13.54	10.39	0.23
C20—C21	1.4065 (3)	1.4065	2.07 (1)	−18.04 (2)	−15.67	−13.00	10.63	0.21
C20—C25	1.3968 (3)	1.3968	2.11 (1)	−18.61 (2)	−16.11	−13.07	10.56	0.23
C21—C22	1.3915 (4)	1.3915	2.13 (1)	−19.97 (2)	−16.57	−13.61	10.20	0.22
C22—C23	1.3980 (4)	1.3980	2.13 (1)	−19.73 (2)	−16.56	−13.57	10.40	0.22
C23—C24	1.3911 (4)	1.3911	2.14 (1)	−20.06 (2)	−16.57	−13.66	10.17	0.21
C24—C25	1.3976 (4)	1.3977	2.11 (1)	−19.07 (2)	−16.28	−13.19	10.40	0.23
C—H‡ (vinyl)	1.10	1.10	1.77 (2)	−16.58 (5)	−16.85	−15.82	16.09	0.07
C—H‡ (H3/H6)	1.10	1.10	1.74 (2)	−16.34 (5)	−16.27	−16.06	15.99	0.02
C—H‡ (methylene)	1.10	1.10	1.73 (2)	−14.93 (5)	−15.99	−15.76	16.82	0.02
C—H‡ (aromatic)	1.08	1.08	1.78 (1)	−16.883 (2)	−17.22	−16.13	16.47	0.07
Ring								
Rh1—C4—C5	–	–	0.74	6.9	–	–	–	–
Six aromatic	–	–	0.19	3.2	–	–	–	–

† R_{ij} is the length of the bond path between atoms. ‡ Average values for C—H bonds of type specified.

density and ellipticity at their b.c.p.s than seen for the other C—C bonds around the cage, indicating a greater π character to the bond. In fact, the values of bond length, $\rho(r)$ and $\nabla^2\rho(r)$ are more consistent with those seen for the delocalized C═C bonds in the aromatic rings.

The bonding situation around rhodium is far more interesting; here the interactions are all closed-shell characterized by small positive values in $\rho(r)$ and positive values for $\nabla^2\rho(r)$. Examining the Laplacian map calculated through Rh1, P1 and Cl1, it can clearly be seen that although the Cl^- ion is almost spherical after the multipole refinement, there is a very small charge concentration directed towards rhodium which is associated with the Rh1—Cl1 interaction, see Fig. 2. This is corroborated by evidence of a small amount of electron density from chlorine in the space between it and the rhodium atom in the deformation-density map, see Fig. 3. On the other hand, the Rh1—P1 interaction is much clearer as there is a significant charge concentration at phosphorus orientated towards the rhodium atom, which is again demonstrated by electron density between the two atoms in the deformation-density map.

Only three b.c.p.s were identified between rhodium and the four C atoms (C1, C2, C4 and C5) of the norbornadiene ligand, which were classified as closed-shell interactions; no b.c.p. was identified between Rh1 and C2. In relation to each of the rhodium–carbon bonds it is noteworthy that the length of the bond path is significantly longer than the interatomic distances, *i.e.* the bond paths are curved. In addition, the ellipticity values ($\varepsilon = \lambda_1/\lambda_2 - 1$) are large owing to the very small value of λ_2 for each Rh1—C bond. Since λ_1 and λ_2 give an indication of the contraction of the electron density perpendicular to the bond path, this suggests that the electron density is fairly flat in one orientation. The stronger *trans* influence of phosphorus compared with chlorine would be expected to weaken bonds *trans* to it, resulting in increased $M—L$ bond lengths compared with those *trans* to chlorine. Indeed the Rh1 to C1/C2 distances are approximately 0.1 Å longer than those to C4/C5. The charge-density analysis also indicates a difference between the Rh1—C1═C2 and Rh1—C4═C5 interactions for several reasons. Firstly, examining the Laplacian maps in Fig. 4 clearly shows that while C1, C4 and C5 have significant charge concentrations orientated towards Rh1, C2 only appears to have a very small charge build up if any at all. Plotting the Laplacian with an increased number of contour levels or from different orientations did not emphasize the charge concentration to a greater extent. Secondly, in the deformation-density plots calculated through the two Rh1—C═C planes (Fig. 5) there is clear evidence of a distortion of the electron density of the C4—C5 bond which is less apparent for the C1—C2 bond, an assertion supported by the higher ellipticity of the former C—C bond (0.36 *versus* 0.26). Finally, as discussed earlier the C═C bonds of the norbornadiene ligand increase in length upon coordination to the rhodium metal centre, however, the C4—C5 bond increased by approximately 0.03 Å more than the C1—C2 interaction. This factor combined with the smaller $\rho(r)$ and $\nabla^2\rho(r)$ values at the C4—C5 b.c.p. indicate that the bond is

Table 3
Comparison of the interatomic distances and angles around the norbornadiene ligand in (1) and as the free ligand (Benet-Buchholz *et al.*, 1998).

Atoms	Bond length in (1) (Å)	Bond length in the free ligand (Å)
C1—C2/ C4—C5	1.385/ 1.416	1.336/ 1.337
C1—C6/ C2—C3/ C3—C4/ C5—C6	1.539/ 1.539/ 1.545/ 1.542	1.536/ 1.537/ 1.534/ 1.537
C3—C7/ C6—C7	1.550/ 1.548	1.554/ 1.555

Atoms	Average angle in (1) (°)	Average angle in the free ligand (°)
C6—C1—C2/C1—C2—C3/ C3—C4—C5/C4—C5—C6	106	107
C2—C3—C4/C5—C6—C1	101	107
C3—C7—C6	94	92

weaker than C1—C2 after coordination probably as a result of the stronger bonding to rhodium, and hence the shorter Rh1—C distances and larger $\rho(r)$ and $\nabla^2\rho(r)$ values at the associated Rh1—C b.c.p.s. At this point it is worth exploring further the differences in the nature of the two Rh1—C═C interactions and the associated lack of Rh1—C2 critical point.

The classical Chatt–Dewar–Duncanson model for bonding between an alkene and a late transition metal describes the interaction through two electron-donation processes: sigma donation from a filled C═C π-orbital into a correctly oriented metal *d* orbital, and π back-bonding from a filled metal *d*-orbital into the empty antibonding C═C π^* orbital. This results in a decrease in the C═C bond order and an associated increase in the bond length. As the extent of π-backbonding increases the bond order decreases and the hybridization of the C atoms can change from sp^2 to sp^3, forming a metallocyclopropane as opposed to a simple alkene adduct. It has been postulated that the pure closed-shell interaction of the alkene adduct would result in a T-shaped interaction, widening to a triangular shape for a metallocyclopropane (Macchi *et al.*, 1998). As Fig. 6 shows all three of the Rh1—C bond paths are concave, indicating that neither interaction is that of an ideal metallocyclopropane (Scherer *et al.*, 2006), however, nor are the interactions consistent with those of a pure T-shaped alkene adduct which have been observed in $[Ag(\eta^2\text{-}C_2H_2)][Al(OC(CH_3)(CF_3)_2)_4]$ (Reisinger *et al.*, 2007).

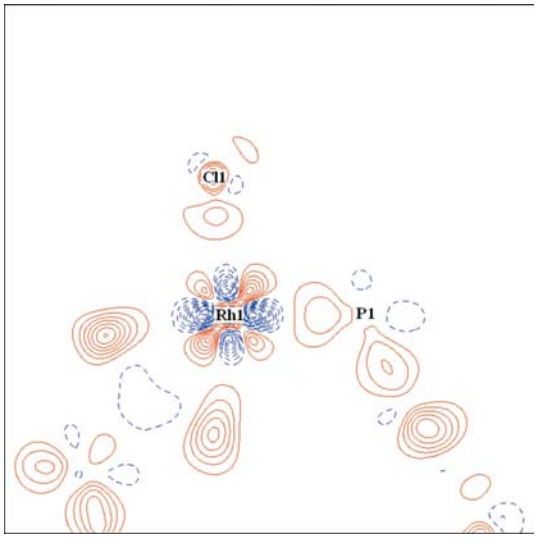

Figure 3
Deformation-density map for (1) after multipole refinement drawn in the plane of Rh1—P1—Cl1. Contours are depicted at the 0.1 e Å^{-3} level, with positive contours as solid red lines and negative contours as blue dashed lines. The zero line is omitted.

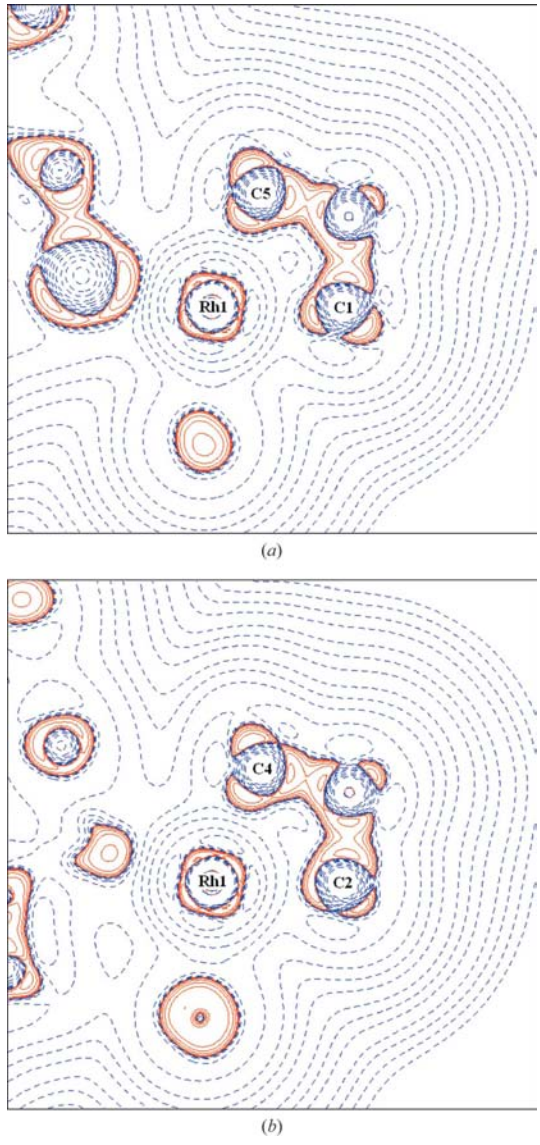

Figure 4
Laplacian of the electron density for (1) drawn in the plane (*a*) Rh1—C1—C5 and (*b*) Rh1—C2—C4. Positive contours are solid red lines, while negative contours are dashed blue lines.

During a charge-density study of [Ni(η^2-C_2H_4)dbpe] (Scherer *et al.*, 2006) noted that the magnitude and orientation of the charge concentrations at the alkene C atoms could give an indication of the hybridization of the C atoms (sp^2 *versus* sp^3). It was noted that as the C atoms became more sp^3 hybridized the metal-directed charge concentration increased and along the alkene bond the bond path became more exocyclic. Examining the Laplacian in the Rh1—C═C planes shows that C4 and C5 have more significant charge concentrations than C1 or C2, suggesting that the hybridization of C4/C5 has more sp^3 character than C1/C2, see Fig. 7. The torsion angles across the C═C bonds of the norbornadiene ligand support this assertion, as the deviation from planarity across C1═C2 is slightly less than that across C4═C5, but more than in the free ligand, see Table 4. This, combined with the fact that the Rh1 to C4 or C5 distances are approximately 0.1 Å shorter than those between Rh1 and C1 or C2, suggests that the interaction of Rh1 with C4═C5 is slightly stronger than that to C1═C2 possibly as a result of the reduced *trans* influence of chlorine compared with phosphorus.

It should also be noted that the Rh1—C1 bond path is significantly more curved (endocyclic) than either of those for Rh1—C4 or Rh1—C5, and that the Rh1—C1 b.c.p. is located near the position where a Rh1—C1—C2 r.c.p. might be expected. In a recent charge-density study of a Co dimer containing alkene fragments bonded to the metal centre (Overgaard *et al.*, 2008), it was noted that the electron density near the centre of the CoC_2 triangles was fairly flat. Since this is the region where the b.c.p.s would be expected, only a slight change in density could cause the b.c.p.s and r.c.p.s to coalesce in a bond catastrophe (Bader, 1990). As shown in Fig. 8 the electron density in the Rh1—C═C planes is very flat, and

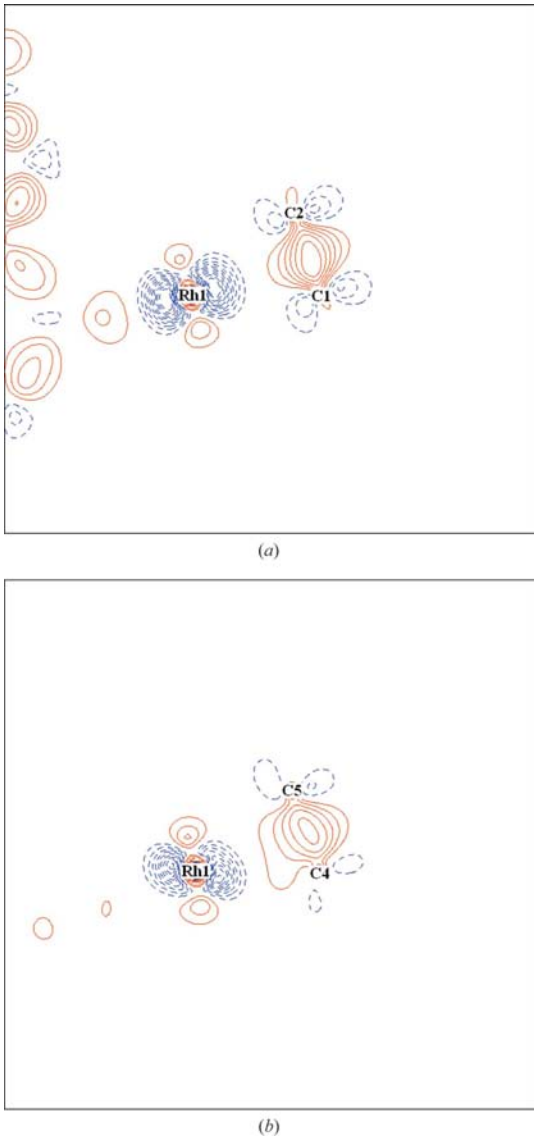

Figure 5
Deformation-density map for (1) after multipole refinement drawn in the plane (*a*) Rh1—C1—C2 and (*b*) Rh1—C4—C5. Contours are depicted at the 0.1 e Å^{-3} level, with positive contours as solid red lines and negative contours as blue dashed lines.

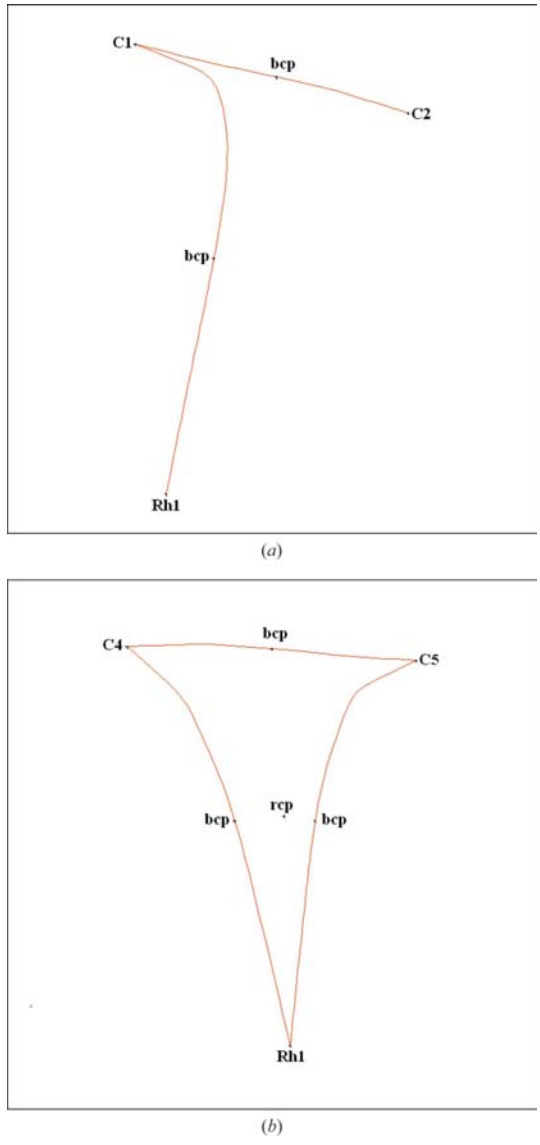

Figure 6
Bond paths between rhodium and the norbornadiene cage with b.c.p.s and r.c.p.s marked for (*a*) Rh1—C1—C2 and (*b*) Rh—C4—C5.

Table 4
Selected *trans* torsion angles across C═C bonds of the norbornadiene cage (Benet-Buchholz *et al.*, 1998).

Atoms	Torsion angle in (1) (°)	Torsion angle in the free ligand (°)
H1—C1—C2—C3	−179 (1)	+176
H2—C2—C1—C6	−165 (1)	−176
H4—C4—C5—C6	+156 (1)	−175
H5—C5—C4—C3	−161 (1)	+177

more so for Rh1—C1═C2, thus it is possible that the lack of Rh1—C2 b.c.p. is due to a bond catastrophe having occurred.

The charges calculated from the multipole refinement (Tables S3 and S4) do show differences between the charges of the C═C carbon atoms on the norbornadiene cage. However, in our opinion these charges are not proven to be a reliable indicator of any particular interaction since a heavy metal atom is involved.

4. Conclusions

The accurate experimental charge-density analysis for [Rh(C_7H_8)(PPh_3)Cl] (1) at 100 K afforded an excellent refinement. All expected b.c.p.s and r.c.p.s were identified in relation to the triphenylphosphine ligand, with both the aromatic C—C and P—C bonds characterized as being shared-shell covalent interactions on the basis of positive values for $\rho(r)$ and large negative values for $\nabla^2\rho(r)$. The topological properties of the C—C bonds around the norbornadiene fragment indicate that these are also shared-shell interactions. Comparison of the bond lengths and angles around the norbornadiene fragment in (1), and those in the free ligand,

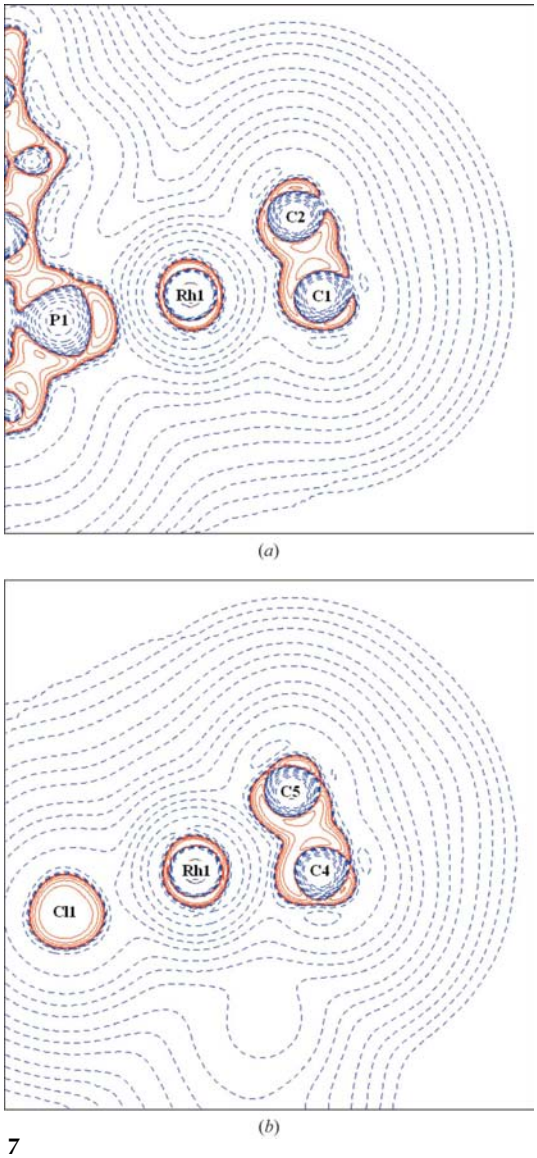

Figure 7
Laplacian of the electron density for (1) drawn in the plane (*a*) Rh1—C1—C2 and (*b*) Rh1—C4—C5, positive contours are solid red lines, while negative contours are dashed blue lines.

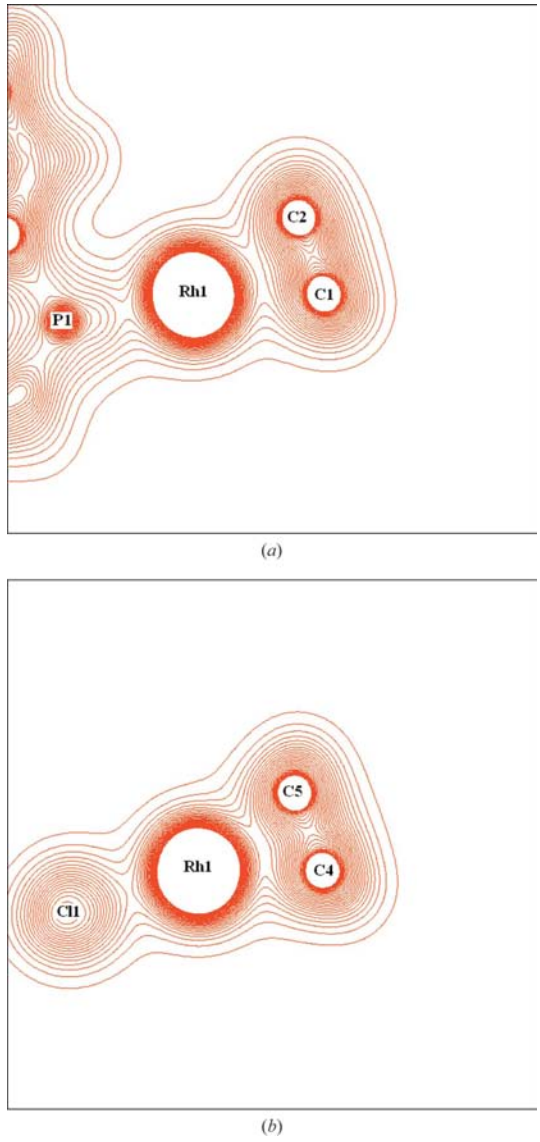

Figure 8
The electron density in the Rh—C═C planes for (*a*) Rh1—C1—C2 and (*b*) Rh1—C4–C5. Contours are depicted at the 0.1 e Å^{-3} level.

indicates that a couple of significant geometric changes occur upon coordination to the metal centre. Firstly the formal double bonds (C1═C2 and C4═C5) increase in length and secondly the C2—C3—C4 and C5—C6—C1 angles reduce by around 6°.

The main reason for carrying out the investigation was to gain insight into the bonding around rhodium. All of the bonds involving rhodium were classified as closed-shell interactions, with small positive values for both $\rho(r)$ and $\nabla^2\rho(r)$. While there was nothing particularly remarkable about either the Rh1—P1 or Rh1—Cl1 bonds, the bonding to the norbornadiene fragment was not quite as expected on simple geometric grounds. The concave nature of the Rh1—C bond paths, charge concentrations at the C atoms of the C═C bonds in norbornadiene and the deviations from planarity across the C═C bonds suggest that the Rh1—C═C interactions are not those of an ideal alkene adduct or metallocyclopropane complex but somewhere in-between. Only three b.c.p.s were identified between Rh1 and the norbornadiene fragment (to C1, C4 and C5), suggesting differences in the Rh1—C1═C2 and Rh1—C4═C5 interactions. It is possible that the lack of Rh1—C2 b.c.p. may be due to a bond catastrophe having occurred or perhaps that the Rh1—C1═C2 interaction has less sp^3 character and is therefore closer to the T-shaped interaction motif of the closed-shell alkene adduct than the Rh1—C4═C5 interaction. Both on geometrical and topological grounds it appears that the Rh1—C4═C5 interaction is stronger than that for Rh1—C1═C2, as expected due to the differing *trans* influence of chlorine and phosphorus, respectively. The differences in bonding for the two Rh1—C═C interactions clearly indicate the importance of charge-density analyses in obtaining a full and clear understanding of the bonding situation in organometallic compounds.

The authors would like to thank the EPSRC for funding.

References

Allen, F. H. (2002). *Acta Cryst.* B**58**, 380–388.

Bader, R. F. W. (1990). *Atoms in Molecules, A Quantum Theory*. Oxford University Press.

Bader, R. F. W. & Essén, H. J. (1984). *J. Chem. Phys.* **80**, 1943–1960.

Benet-Buchholz, J., Haumann, T. & Boese, R. (1998). *Chem. Commun.* pp. 2003–2004.

Bennett, M. A. & Wilkinson, G. (1961). *J. Chem. Soc.* pp. 1418–1420.

Blessing, R. H. (1997). *J. Appl. Cryst.* **30**, 421–426.

Brayshaw, S. K., Sceats, E. L., Green, J. C. & Weller, A. S. (2007). *Proc. Natl. Acad. Sci.* **104**, 6921–6926.

Chatt, J. & Duncanson, L. A. (1953). *J. Chem. Soc.* pp. 2939–2947.

Crabtree, R. H. (2005). *The Organometallic Chemistry of the Transition Metals*. Hoboken, NJ: Wiley.

Dewar, M. J. S. (1951). *Bull. Soc. Chim. Fr.* pp. C71–C79.

Eickerling, G., Mastalerz, R., Herz, V., Scherer, W., Himmel, H.-J. & Reiher, M. (2007). *J. Chem. Theory Comput.* **3**, 2182–2197.

Farrugia, L. J. (1999). *J. Appl. Cryst.* **32**, 837–838.

Hansen, N. K. & Coppens, P. (1978). *Acta Cryst.* A**34**, 909–921.

Hirshfeld, F. L. (1976). *Acta Cryst.* A**32**, 239–244.

Jun, C. H. (2004). *Chem. Soc. Rev.* **33**, 610–618.

Macchi, P. & Coppens, P. (2001). *Acta Cryst.* A**57**, 656–662.

Macchi, P., Proserpio, D. M. & Sironi, A. (1998). *JACS*, **120**, 1447–1455.

Nonius (1999). *Collect.* Nonius BV, Delft, The Netherlands.

Otwinowski, Z. & Minor, W. (1997). *Methods in Enzymology*, Vol. 276, *Macromolecular Crystallography*, edited by C. W. Carter Jr & R. M. Sweet, Part A, pp. 307–326. New York: Academic Press.

Overgaard, J., Clausen, H. F., Platts, J. A. & Iversen, B. B. (2008). *JACS*, **130**, 3834–3843.

Reisinger, A., Trapp, N., Krossing, I., Altmannshofer, S., Herz, V., Presnitz, M. & Scherer, W. (2007). *Angew. Chem. Int. Ed.* **46**, 8295–8298.

Rybtchinski, B. & Milstein, D. (1999). *Angew. Chem. Int. Ed.* **38**, 870–883.

Scherer, W., Eickerling, G., Shorokhov, D., Gullo, E., McGrady, G. S. & Sirsch, P. (2006). *New J. Chem.* **30**, 309–312.

Sheldrick, G. M. (2008). *Acta Cryst.* A**64**, 112–122.

Su, Z. & Coppens, P. (1998). *Acta Cryst.* A**54**, 646–652.

Takenaka, Y. & Osakada, K. (2000). *Bull. Chem. Soc. Jpn*, **73**, 129–130.

Volkov, A., Macchi, P., Farrugia, L. J., Gatti, C., Mallinson, P., Richter, T. & Koritsanszky, T. (2006). *XD*2006. University at Buffalo, State University of New York, NY, USA; University of Milano, Italy; University of Glasgow, Scotland; CNRISTM, Milano, Italy, Middle Tennessee State Unviersity, TN, USA.